Phys. Lett. B 862 (2025) 139353

Contents lists available at ScienceDirect

Physics Letters B

journal homepage: www.elsevier.com/locate/physletb

Letter

Systematic studies to produce heavy above-target nuclides in multinucleon transfer reactions

H.M. Devaraja [a,b,*], A.V. Yeremin [a,c,1], M.L. Chelnokov [a], V.I. Chepigin [a], S. Heinz [d], A.V. Isaev [a,c], I.N. Izosimov [a], Sh.A. Kalandarov [a], A.V. Karpov [a,c], D.E. Katrasev [a], A.A. Kuznetsova [a], O.N. Malyshev [a,c], R.S. Mukhin [a], A.G. Popeko [a,c], Yu.A. Popov [a,c], V.V. Saiko [a,e], B. Sailaubekov [a,b,f], E.A. Sokol [a], A.I. Svirikhin [a,c], M.S. Tezekbayeva [a,b,c,e], U.A. Abitayeva [b], E.K. Almanbetova [a,b], A.A. Almas [b], A.K. Azhibekov [a,b], M.A. Bychkov [a], O. Dorvaux [g], B. Gall [g], K. Hauschild [h], K. Kessaci [g], A. Lopez-Martens [h], E.V. Mardyban [a,c,b], K. Mendibayev [a,b,e], Zh.Ye. Nakypbek [b], B.A. Urazbekov [b,f]

[a] Joint Institute for Nuclear Research, 141980, Dubna, Russia
[b] Korkyt Ata Kyzylorda University, N01P2T6, Kyzylorda, Kazakhstan
[c] Dubna State University, 141982, Dubna, Russia
[d] GSI Helmholtzzentrum für Schwerionenforschung GmbH, 64291, Darmstadt, Germany
[e] Institute of Nuclear Physics, 050032, Almaty, Kazakhstan
[f] L.N. Gumilyov Eurasian National University, Astana, Kazakhstan
[g] Université de Strasbourg, CNRS, IPHC, Strasbourg, UMR7178, 67037, France
[h] IJCLab, IN2P3-CNRS, Université Paris-Saclay, Orsay, UMR9012, 91405, France

ARTICLE INFO

Editor: B. Blank

Keywords:
Multinucleon transfer (MNT) reaction
Heavy and superheavy nuclei
α-spectra

ABSTRACT

We present studies of multinucleon transfer reactions in collisions of ^{48}Ca+^{208}Pb, ^{50}Ti+^{208}Pb, and ^{40}Ar+^{209}Bi which lead to the population of nuclei with proton numbers greater than the target proton number. The target-like reaction products were separated in flight using the velocity filter SHELS of the Flerov Laboratory for Nuclear Reactions (FLNR), Dubna. Our goal was to examine transfer reactions for producing new heavy and superheavy nuclei and to assess the applicability of velocity filters for their investigation. We observed and studied about 40 different nuclides, resulting from the transfer of up to eight protons from the projectile to the target and moving in forward direction relative to the beam axis. We present cross-section systematics for isotopes of elements Z = (83 – 91) measured in our experiment and compare them with available data from transfer reactions with actinide targets which lead to isotopes up to Z = 103.

1. Introduction

Most of the presently known transuranium nuclides, including the region of superheavy elements, were discovered in heavy ion fusion reactions. Meanwhile, this conventional synthesis method is reaching its experimental limitations. Heavy ion fusion reactions employ naturally available stable projectiles incident on target nuclei, up to the heaviest available Einsteinium (Z = 99). With this, fusion products are neutron-deficient because of the curvature of the valley of stability in the N-Z plane.

The discovery of still unknown neutron-rich nuclides in the heavy and superheavy element region could be achieved through the use of multinucleon transfer (MNT) reactions, which are considered to be a potential method, according to successful experimental results [1–20] and theoretical calculations [21–36].

MNT reactions revealed already their potential to discover new isotopes. Between 1969 and 1995, about 75 new neutron-rich nuclides were discovered [37]. JINR Dubna, Orsay in France, LBNL and GSI are the places where the majority of these discoveries took place. These labs employed mainly the Bρ-ΔE-E and TOF-ΔE-E methods to identify the

* Corresponding author at: Joint Institute for Nuclear Research, 141980, Dubna, Russia.
E-mail address: devaraja@jinr.ru (H.M. Devaraja).
[1] Alexander Vladimirovich Yeremin passed away on 22 July 2024.

https://doi.org/10.1016/j.physletb.2025.139353
Received 17 October 2024; Received in revised form 24 February 2025; Accepted 24 February 2025
Available online 25 February 2025

reaction products, resulting in mass and charge resolutions of about 1%. This prevents the identification of nuclei with mass numbers A > 200. Until today the primary method to identify and investigate heavier MNT products is decay spectroscopy after separation of the nuclei from primary beam and background events.

MNT reactions were also successfully applied in the transactinide region using projectiles that range from carbon (C) to uranium (U) incident on the heaviest available actinide targets: ^{238}U, ^{244}Pu, ^{248}Cm, ^{249}Cf, and ^{254}Es [2–7,9,12]. In these experiments, radiochemical separation followed by decay spectroscopy has been used for the investigation of several nuclides up to lawrencium (Lr). MNT products with cross-sections as low as 20 nb were observed. Some of these experiments were also successful in discovering new isotopes, such as ^{238}Th in the ^{18}O+^{238}U reaction [38], ^{243,244}Np in the ^{136}Xe+^{244}Pu reaction [10], and ^{260}Md in the ^{18}O+^{254}Es reaction [39]. Radiochemical methods have the capability of 4π collections of MNT products, but they are not fast enough to detect exotic nuclides with half-lives of less than a few minutes.

In more recent years, using the velocity filter SHIP, MNT reactions such as ^{58,64}Ni+^{207}Pb [14,15], ^{48}Ca + ^{248}Cm [16,18], and ^{48}Ca + ^{238}U [19] have been investigated. A large region of populated MNT products below and above the target has been identified. Their isotopic distribution, excitation energy, and the influence of nuclear shells on the populated nuclides were studied. In the ^{48}Ca+^{248}Cm reaction, using the α-α correlation method, cross-sections on the 1 nb scale were reached. This led to the identification of several new neutron-deficient transuranium isotopes [16] and to the observation of the so far heaviest MNT product ^{260}No [18]. However, MNT reactions at Coulomb barrier energies result in large angular distributions of their products and small efficiencies of less than 1% for inflight separation with the velocity filter SHIP.

Available theoretical and experimental results indicate that cross-sections on the scale of nanobarn and below are expected for new MNT products beyond uranium. Therefore it is crucial for future experiments to choose reaction systems and energies which lead to largest possible cross-sections and to apply efficient separation and identification methods capable of detecting single events, akin to those used for discovering exotic heavy and superheavy nuclei.

In this work we focus on the synthesis of MNT products with proton numbers greater than the target proton number, in the following denoted as “above-target” MNT products. A good testing ground for systematic studies and a proof-of-principle are reactions using Pb or Bi targets because corresponding above-target MNT products are located in a wide region of α emitters which facilitates their identification.

We present new data on MNT reactions from collisions of ^{48}Ca+^{208}Pb, ^{50}Ti+^{208}Pb, and ^{40}Ar+^{209}Bi measured at the velocity filter SHELS [40]. We focus on the study of cross-section trends for above-target MNT products measured with Pb, Bi targets and with actinide targets. Also, we compare data measured in radiochemical experiments with data obtained by using in-flight separation with a velocity filter.

2. Experiment

The beams of ^{48}Ca, ^{50}Ti, and ^{40}Ar were delivered from the U400 cyclotron of FLNR. Table 1 provides information on the investigated reactions and related parameters. The Bi_2O_3 targets for the ^{40}Ar+^{209}Bi reaction had a thickness of 526 μg/cm^2 and were electrodeposited onto a 1.5 μm thick Ti foil. In the ^{50}Ti+^{208}Pb and ^{48}Ca+^{208}Pb studies, the targets consisted of ^{208}PbS layers with thicknesses of 500 μg/cm^2 and 437 μg/cm^2, respectively, electrodeposited onto 1.5 μm thick Ti foils.

The velocity filter SHELS was used for inflight selection of target-like MNT products moving at forward angles of ±4 degrees with respect to the beam axis. Depending on the projectile-target combination and beam energy, the measured target-like transfer products had velocities ranging around approximately 1.5 times the compound system velocity v_{CS}. This value was obtained by adjusting the electric and magnetic fields of SHELS in incremental steps to select and transmit reaction products within the velocity window $(1.1-1.8)\,v_{CS}$. Reaction products with other velocities were stopped by the beam stopper.

Table 1
The investigated reactions are listed along with the corresponding parameters. E_{lab} represents the laboratory energy at the middle of the target, E_{CM} denotes the corresponding center of mass energy, and E/B_{int} indicates the ratio of the beam energy to the Bass interaction barrier [41]. I_{beam} is the beam intensity and d_{target} the target thickness.

	^{40}Ar+^{209}Bi	^{50}Ti+^{208}Pb	^{48}Ca+^{208}Pb
E_{lab} [MeV]	194.3	242.8	236.0
E_{CM} [MeV]	163.1	195.7	191.8
E/B_{int}	0.99	1.00	1.09
I_{beam} [pμA]	0.125	0.05	0.280
d_{target} [μg/cm^2]	526±100	500±40	437±13
Measurement time [h]	18	11.4	42

The selected reaction products pass through the TOF detectors behind SHELS and are finally implanted in a double-sided silicon strip detector (DSSD) where the energy, time and position of the implanted nuclei and their decay products is measured. SHELS employs a highly pixelated 100×100 mm^2 DSSD with 128 vertical and horizontal strips, this yields 16384 different pixels for genetic position and time correlations between DSSD signals. In addition, eight 50×60 mm^2 silicon tunnel detectors (700 μm thick) are positioned in the backward hemisphere to register α particles or fission fragments which are emitted in the backward direction. This setup allows to reconstruct the decay properties of the implanted reaction products and with this, their identification. The signals produced in the TOF detectors allow to distinguish between signals in the DSSD, which are coincident and correspond to the implantation of reaction products and those, which are not and correspond to the α decay of the implanted species. To distinguish directly populated MNT products from nuclei populated by precursor decays, we used the recoil-α and α-α correlation method. The literature data on decay energy, half-life, and branching ratios were sourced from [42].

3. Results and discussion

3.1. MNT reactions with Pb and Bi targets

3.1.1. Observed isotopes and cross-sections

The α spectra measured in reactions of ^{50}Ti+^{208}Pb and ^{40}Ar + ^{209}Bi are presented in Fig. 1. They reveal various strongly populated nuclides beyond the target nuclei Pb and Bi. Further, rarely populated nuclides we observed by using the recoil-α and α-α correlation method for suppression of background events. The measured velocity spectra of the nuclei reveal that all of them result from nucleon transfer reactions. The collection of identified above-target MNT products from the three reactions is shown in Fig. 2. Isotopes with up to eight protons and seven neutrons more than the respective target nucleus are observed. Here one must stress, that the observed MNT product neutron number includes both, the net number of transferred neutrons and the neutrons evaporated from the excited primary MNT products. The excitation energies of MNT products and the resulting evaporation of neutrons from the primary MNT products are discussed in the next subsection.

The cross-sections of directly populated transfer products are shown in Fig. 3 as a function of the isotope mass number A. In the following we denote this kind of representation as ‘isotopic distribution’. The cross-sections in Fig. 3 are differential cross-sections corresponding to SHELS acceptance angle of 15 msr. The lowest measured cross-sections were at the level of 50 pb/sr, reached in five hours of data collection at the respective velocity setting, beam intensity and target thickness.

To obtain total cross-sections, we determined the angular efficiency of SHELS for MNT products in frame of theoretical calculations using

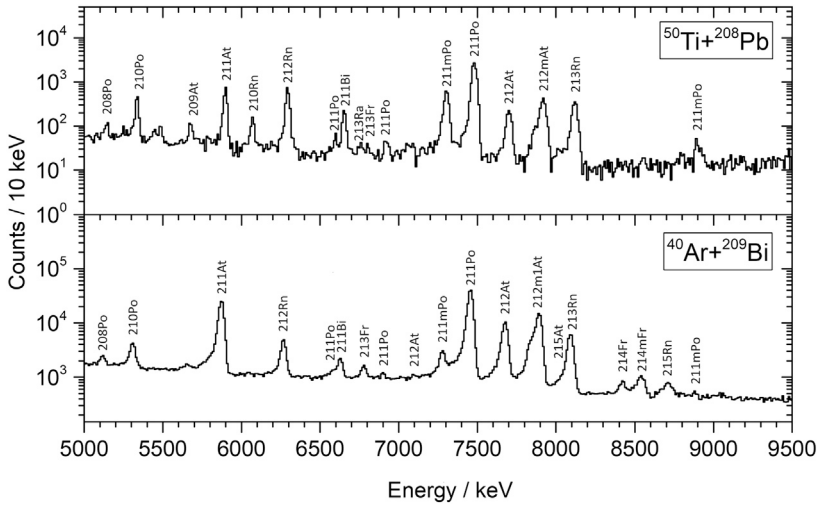

Fig. 1. Measured α-spectra of the target-like transfer products from the ^{50}Ti+ ^{208}Pb and ^{40}Ar+ ^{209}Bi reactions. The spectrum was accumulated over 11.4 hours for the transfer reaction products from ^{50}Ti+ ^{208}Pb, and over 18 hours for those from the ^{40}Ar+ ^{209}Bi reaction.

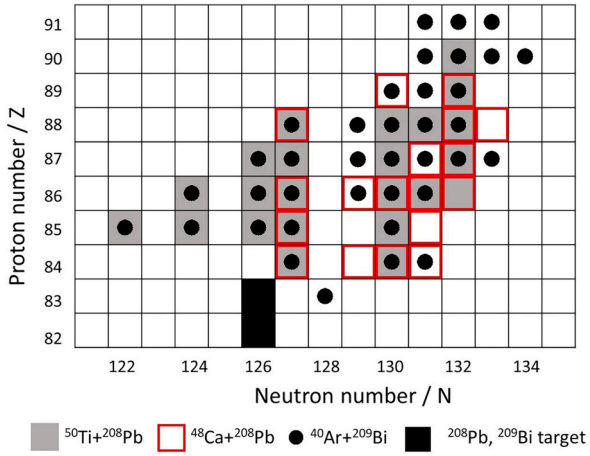

Fig. 2. The nuclear chart shows the region of identified nuclides from the reactions ^{50}Ti+ ^{208}Pb (gray filled squares), ^{48}Ca+ ^{208}Pb (red open squares), and ^{40}Ar+ ^{209}Bi (black solid circles). The filled black squares indicate the positions of the ^{208}Pb and ^{209}Bi targets.

the Langevin model. Angular distributions for MNT products up to Ra, emerging from Ca+Pb collisions are shown in Fig. 4. The calculations indicate that, on average, only 5% of the populated nuclides move at forward angles of ±4 degrees which corresponds to the opening angle of SHELS. The remaining 95% of the MNT products are emitted at angles greater than ±4 degrees. Taking also into account the 10% transmission efficiency of SHELS, only ∼0.5% of the above-target MNT products were detected. The differential limit cross-section of 50 pb/sr corresponds to a total limit cross-section of ∼1 nb.

The maxima of the isotopic distributions are found for MNT products with neutron-to-proton ratios N/Z very close to the one of the entrance channel system (see Fig. 3). The N/Z values of Ar+Bi and Ti+Pb are 1.47 and 1.48, respectively. These numbers agree with the N/Z where the respective isotopic distributions peak. The same is observed for Ca+Pb collisions where the isotopic distributions peak around N/Z = 1.51 in agreement with the N/Z of Ca+Pb.

The cross-sections measured in ^{48}Ca+ ^{208}Pb collisions are about one to two orders of magnitude smaller in comparison to the other two reactions. One factor is the beam energy, which was in Ca+Pb 9% higher than the Bass barrier while in the other two reactions the beam energy was at the Bass barrier. Another possible explanation might be that ^{48}Ca as well as ^{208}Pb are both doubly magic nuclei. MNT reactions in such doubly magic systems might be hindered because both nuclei loose their doubly magic configuration after a transfer of nucleons. In addition, the proton and neutron transfer probabilities from the projectile to the target nucleus depend on the corresponding separation energies and Q values. Although the neutron separation energies from the projectile nuclei and the Q values for 1n transfer change slightly in these three reactions, the proton separation energy and the Q value for 1p transfer are much larger in the Ca+Pb reaction compared to the other two reactions. This difference may contribute to the greater hindrance observed in nucleon transfer for the Ca+Pb reaction. Furthermore, the analysis of the potential energy surface in the N-Z plane using the macro-microscopic approach [43] indicates the strong presence of N/Z equilibration in the ^{40}Ar+ ^{209}Bi and ^{50}Ti+ ^{208}Pb systems, in comparison to the ^{48}Ca+ ^{208}Pb systems. This process leads to increase in cross-sections of target-like transfer products in these two reactions compared to ^{48}Ca+ ^{208}Pb reaction.

3.1.2. MNT product excitation energies

Beside isotopes of Bi and Po, the observed MNT products result from deep inelastic reactions with full dissipation of the kinetic energy. We obtained this information from the velocities of the detected target-like MNT products and by assuming a binary reaction process like described in ref. [14]. The dissipated energy is transformed to excitation energy and deformation of the primary MNT products. We derived the excitation energies of the primary target-like MNT products by regarding the reaction Q-values. Transfer reactions which increase the mass to charge asymmetry of the two involved nuclei are connected with negative Q-values. This is the case in our experiments when we create above-target MNT products.

We assumed that the yields of the primary transfer products are given by the reaction Q-value and that isotopes connected with the least negative Q-values are the most likely primary MNT products. The difference, D_n, between the MNT product neutron number at the Q-value peak (fitted with a Gaussian to obtain the peak maximum in this work) and the neutron number at the peak of the measured isotopic distribution indicates the average number of neutrons evaporated from the primary products. We assumed that approximately 10 MeV is required to evaporate a neutron. This number includes the neutron separation energies of typically (7 − 8) MeV in the region above Pb and the kinetic energy of a neutron within the nucleus, based on the peak of the Boltzmann distribution, which is around 1.7 MeV. The excitation energy is then $E^* = D_n \times 10$ MeV.

We found that the above-target MNT products from all reaction systems have excitation energies of ∼20 MeV or less. It means that they

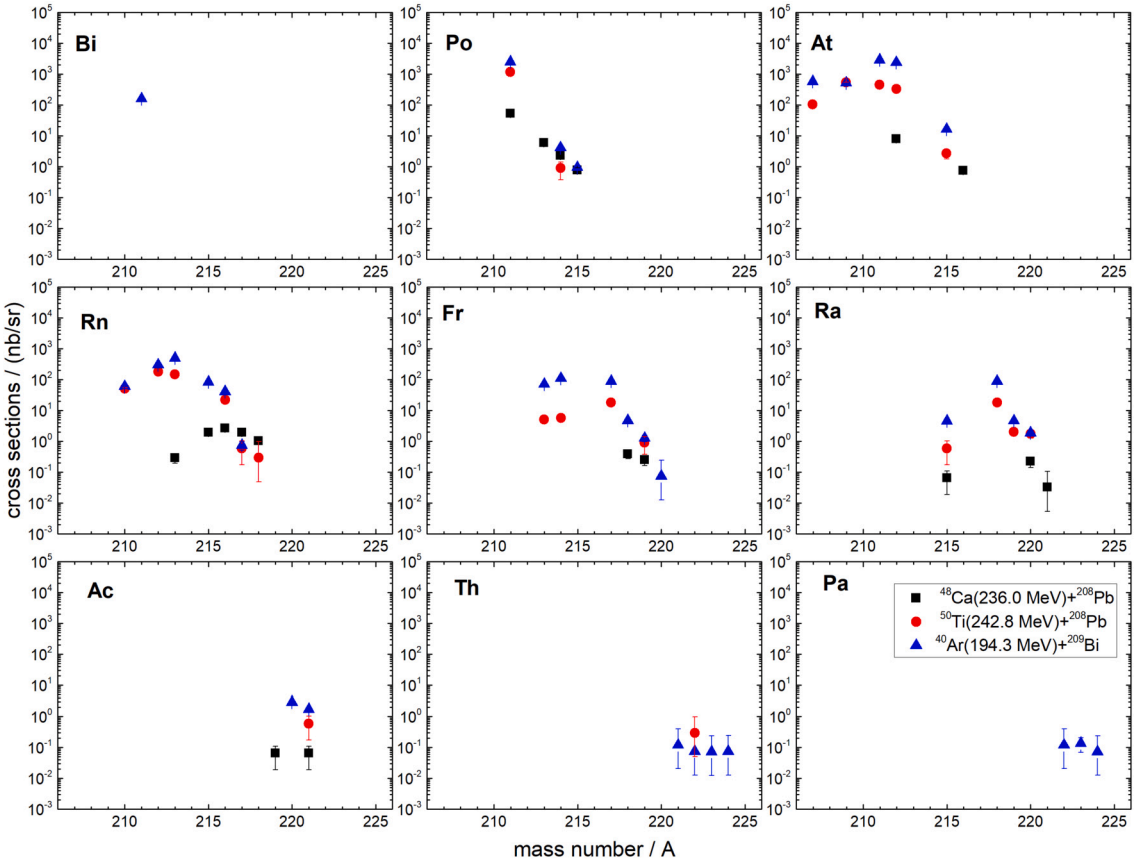

Fig. 3. Production cross-sections are shown as a function of mass number A for the isotopes of elements ranging from Bi to Pa. These correspond to the directly populated target-like transfer products in the ^{48}Ca+ ^{208}Pb, ^{48}Ti+ ^{208}Pb, and ^{40}Ar+ ^{209}Bi reactions.

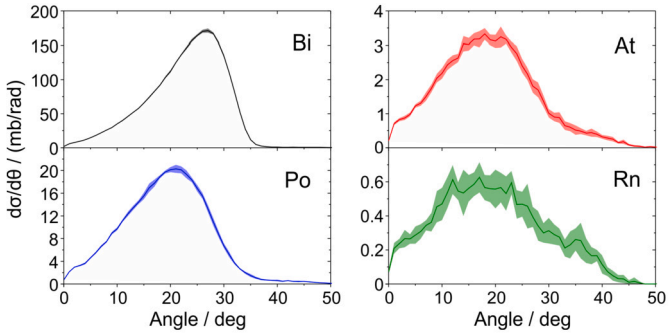

Fig. 4. Estimated angular distributions using the dynamical model based on the Langevin equations for the ^{48}Ca+ ^{208}Pb at a lab energy of 236 MeV.

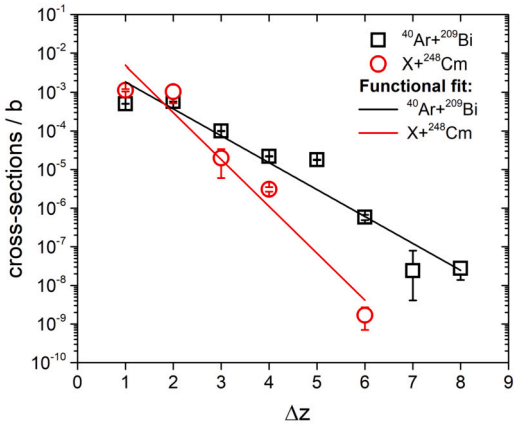

Fig. 5. Measured total cross-sections of above-target MNT products as a function of the net number of transferred protons, ΔZ. Data are shown for reactions of ^{40}Ar + ^{209}Bi and reactions with different projectile nuclei (denoted by X) on ^{248}Cm targets [2–5,18]. The denoted cross-sections belong to the maxima of the respective isotopic distributions.

result after the evaporation of up to two neutrons from the primary MNT products. It is noteworthy that also MNT products from collisions of Ca + Pb, which took place at a beam energy of 9% above the barrier, reveal the same low excitation energies.

3.2. Comparison to MNT reactions with actinide targets

If we want to enter the transuranium or even superheavy element region, we have to use actinide targets. MNT reactions with actinides from Cm to Es and diverse projectiles were investigated in a series of early experiments using radiochemical techniques for isotope separation and identification. Also at the velocity filter SHIP of GSI MNT products emerging from reactions of Ca + Cm were studied. In the following we will compare the characteristics of above-target MNT products from reactions with Pb, Bi and with actinide targets.

Also in reactions with actinide targets the maximum cross-sections are measured for MNT products with N/Z equal to the N/Z of the entrance channel system. Due to the larger number of neutrons in that systems, N/Z ≈1.54 and with that ∼5% larger compared to reactions with Pb targets.

Fig. 5 shows the measured total cross-sections of above-target MNT products as a function of the net number of transferred protons, ΔZ. Data are shown for reactions of Ar + Bi and reactions with Cm targets. The denoted cross-sections belong to the maxima of the respective isotopic

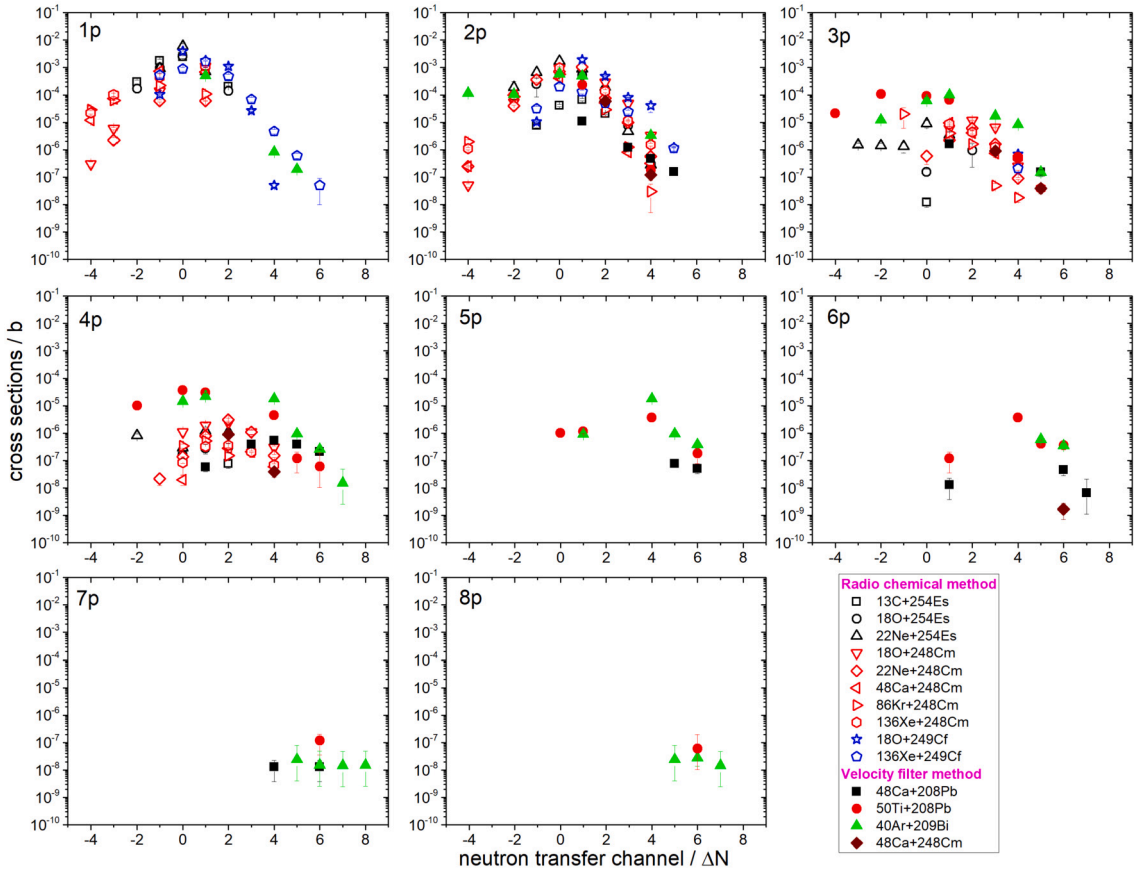

Fig. 6. Measured cross-sections of above-target MNT products from different proton transfer channels as a function of the difference, ΔN, between the target nucleus neutron number and the MNT product neutron number. The value of ΔN includes the net number of transferred neutrons and the number of evaporated neutrons. The data from this work, obtained with velocity filter SHELS, along with data from the velocity filter SHIP for the reaction ^{48}Ca + ^{248}Cm [18], are compared with results from various reactions measured in radiochemical experiments with actinide targets ^{248}Cm, ^{249}Cf, and ^{254}Es. Radiochemical data include reactions of ^{13}C [12], ^{18}O [6] and ^{22}Ne [6] projectiles were incident on ^{254}Es targets, ^{18}O [3], ^{22}Ne [2], ^{48}Ca [4], ^{86}Kr [5], and ^{136}Xe [5] projectiles were incident on ^{248}Cm targets, and ^{18}O [3] and ^{136}Xe [9] projectiles were incident on ^{249}Cf targets, all at or near the Coulomb barrier.

distributions. In both above-target regions we observe a cross-section decrease with increasing number of protons moving from the projectile to the target nucleus. The curves diverge with increasing ΔZ. We account this to the larger fissility of the heavier nuclei. With Cm targets we are entering the sub-nanobarn region if we transfer ≥ 6 protons.

Fig. 6 shows the measured total cross-sections of above-target MNT products as a function of the difference ΔN between the target nucleus neutron number and the MNT product neutron number. The value of ΔN includes the net number of transferred neutrons as well as the number of evaporated neutrons. Each graph in Fig. 6 belongs to a fixed number of transferred protons, ΔZ. The figures contain all available data on above-target MNT products measured in radiochemical experiments and at the velocity filters SHELS and SHIP with a large variety of projectile-target combinations.

In radiochemical experiments the lowest measured cross-sections were about 20 nb. Despite using very heavy targets such as Cm (Z = 96), Cf (Z = 98), and Es (Z = 99), only the population of nuclides up to the 4p transfer channels have been observed. Specifically, with Cm targets nuclides up to Fm (Z = 100) were observed; with Cf targets nuclides up to No (Z = 102), and with Es targets nuclides up to Lr (Z = 103). Despite using various projectiles on different targets, the isotopic distributions from 1p to 4p transfer channels are comparable within one order of magnitude. In experiments of ^{48}Ca + ^{248}Cm at the velocity filter SHIP (sensitivity 1 nb) isotopes up to No (Z = 102) were observed, which corresponds to the 6p channel. MNT products which result from a transfer of more than 6 protons are only observed in the above-Pb region.

3.3. Future prospects for MNT reactions at in-flight separators

The smallest MNT product cross-sections were measured in experiments using in-flight separation with velocity filters. The data from SHELS and SHIP are in good agreement. The estimated yield per day (in logarithmic scale) at the present velocity filters is shown in Fig. 7 for the parameters provided in the figure caption. The estimation is based on cross-section calculations using Langevin-type dynamical model for the ^{48}Ca + ^{251}Cf reaction at E_{lab} = 293 MeV [44]. These estimations revealed that several neutron-rich unknown transuranium isotopes, extending up to the superheavy region with Z = 108, can be produced with cross-sections greater than 1 nb. About 15 still unknown nuclides are situated between the region of nuclei discovered in cold and hot fusion reactions. These isotopes can potentially be observed using MNT reactions at the present velocity filters.

Additionally, around 50 still unknown neutron-rich nuclides in the transuranium region, directly joining the known region, are expected to be produced with sufficient yields to study them at the current velocity filters. The methods employed at Ref. [18], including decay activities, total TKE distributions of the fission fragments, and the magnetic rigidities of the populated nuclei, combined with optimized separator tuning, will be beneficial to identify the majority of these isotopes.

A disadvantage of velocity filters is their small angular and energy acceptance, which is on the scale of few percent or less at presently existing devices. Another restriction concerns the choice of collision system. At velocity filters, the separation of the primary beam from target-like re-

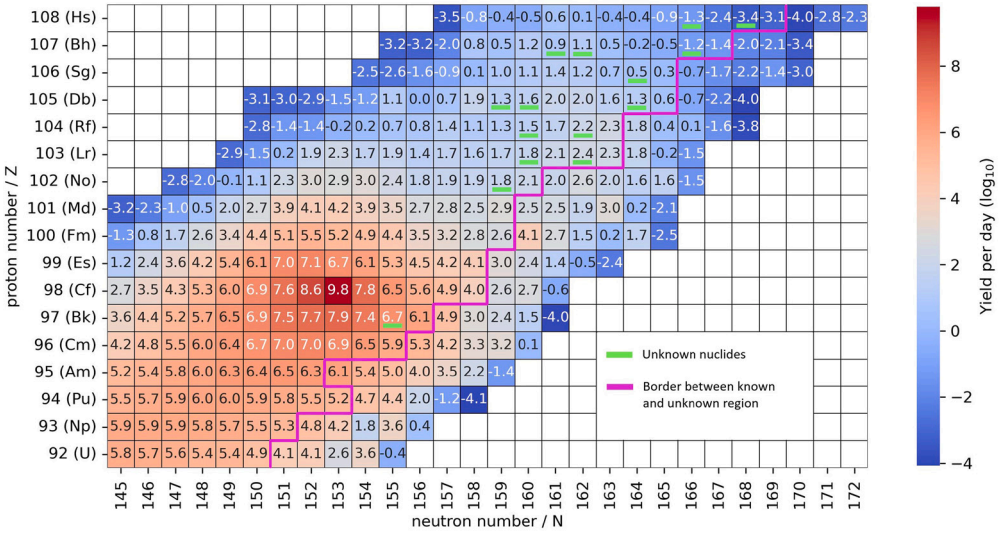

Fig. 7. The estimated yield per day at the velocity filters, based on cross-section calculations using Langevin-type dynamical model for the ^{48}Ca + ^{251}Cf reaction, at E_{lab} = 293 MeV, is presented. The following realistic values were considered: a ^{48}Ca beam intensity (I_{beam}) of 1.2 pμA, a ^{251}Cf target thickness (D_t) of 500 μg/cm^2, and an efficiency of 1% for an ideal experimental case with optimized field settings. The solid magenta line represents the boundary between the already discovered region of nuclides and the yet-to-be-discovered region. Within the discovered region, 15 nuclides, marked in green, are yet to be found and are situated between regions of nuclides discovered through cold and hot fusion reactions.

action products becomes increasingly challenging with increasing symmetry of the collision system. As a result, reactions involving symmetric systems like Xe + U, or uranium beams on actinide targets are difficult to investigate, but might be an interesting option according to multidimensional dynamical model calculations based on Langevin equations [29].

4. Conclusions and outlook

Multinucleon transfer reactions remain the only method to access the neutron-rich transuranium region, and as demonstrated in this work, in-flight separators are a potential method for these studies. The investigation of above-target MNT products using the velocity filter SHELS has demonstrated the potential of this method to observe rare, heavy MNT products. Although SHELS is not a dedicated facility for studying MNT reactions, it has proven to be sensitive to measure MNT products with cross-sections down to 1 nb, more than an order of magnitude smaller than those reached with other techniques. The same sensitivity was reached in previous experiments with the GSI velocity filter SHIP. Our results are a proof of principle.

With the future upgrade of the Dubna U400 cyclotron, the beam intensity is expected to be about three times higher than that of the current U400. By utilizing these increased intensities and further optimizing the field settings of the velocity filter, we expect a sensitivity on the order of 0.1 nb. This could enable the identification of MNT products from even more proton and neutron transfer channels leading to above-target MNT products.

We studied cross-sections of above-target MNT products using ^{208}Pb/^{209}Bi targets with those using ^{248}Cm targets. Like expected, in both cases the cross-sections drop with increasing number of transferred protons. But the drop is steeper in the above-Cm region. The cross-sections of the 6p transfer channels measured with Pb and with Cm targets reveal a difference of two orders of magnitude. If we extend the observed trend to the 8p channel, using ^{248}Cm targets we can expect cross-sections close to 10 pb for isotopes of the element rutherfordium. If the heavier ^{251}Cf or ^{254}Es targets are used instead of ^{248}Cm, the 8p channel could potentially lead to the synthesis of isotopes of elements with Z = 106 and 107, respectively. For above-Pb as well as above-Cm MNT products, the maximum cross-sections are found for isotopes in the beta stability valley. Toward the neutron-rich side, cross-sections drop by about one order of magnitude for every additional neutron.

At FLNR, the dedicated Separator for TransActinide Research (STAR) is currently under construction alongside the modernization of the U400 cyclotron (U400R) [45]. STAR will be a kinematic separator, developed for high intensity, high background suppression, and increased transmission of fusion and transfer reaction products. This facility will be particularly beneficial as it allows for the analysis of MNT products at different angles. Beside decay tagging, STAR will also allow the identification of nuclei by precise mass measurements with a penning trap or multiple reflection time-of-flight spectrometer [46]. This will be advantageous for the neutron-rich transuranium region, where the majority of populated nuclei are expected to be β emitters or α/SF decaying with long half-lives.

Declaration of competing interest

The authors declare that they have no known competing financial interests or personal relationships that could have appeared to influence the work reported in this paper.

Acknowledgement

We gratefully acknowledge the support of this project by grants of the Science Committee of the Ministry of Science and Higher Education of the Republic of Kazakhstan (Grant No. AP19577048). We also acknowledge the support of the French National Research Agency contract project ANR-06-BLAN-0034-01. We would like to thank the crew of the U400 accelerator for the excellent technical support throughout the experiments.

Data availability

Data will be made available on request.

References

[1] M. Schädel, et al., Isotope distributions in the reaction of ^{238}U with ^{238}U, Phys. Rev. Lett. 41 (1978) 469–472, https://doi.org/10.1103/PhysRevLett.41.469.
[2] D. Lee, et al., Production of heavy actinides from interactions of ^{16}O, ^{18}O, ^{20}Ne, and ^{22}Ne with ^{248}Cm, Phys. Rev. C 25 (1982) 286–292, https://doi.org/10.1103/PhysRevC.25.286.

[3] D. Lee, et al., Excitation functions for production of heavy actinides from interactions of ^{18}O with ^{248}Cm and ^{249}Cf, Phys. Rev. C 27 (1983) 2656–2665, https://doi.org/10.1103/PhysRevC.27.2656.

[4] D.C. Hoffman, et al., Excitation functions for production of heavy actinides from interactions of ^{40}Ca and ^{48}Ca ions with ^{248}Cm, Phys. Rev. C 31 (1985) 1763–1769, https://doi.org/10.1103/PhysRevC.31.1763.

[5] K.J. Moody, et al., Actinide production in reactions of heavy ions with ^{248}Cm, Phys. Rev. C 33 (1986) 1315–1324, https://doi.org/10.1103/PhysRevC.33.1315.

[6] M. Schädel, et al., Transfer cross sections from reactions with ^{254}Es as a target, Phys. Rev. C 33 (1986) 1547–1550, https://doi.org/10.1103/PhysRevC.33.1547.

[7] M. Schädel, et al., Actinide production in collisions of ^{238}U with ^{248}Cm, Phys. Rev. Lett. 48 (1982) 852–855, https://doi.org/10.1103/PhysRevLett.48.852.

[8] H. Gäggeler, et al., Production of cold target-like fragments in the reaction of ^{48}Ca+^{248}Cm, Phys. Rev. C 33 (1986) 1983–1987, https://doi.org/10.1103/PhysRevC.33.1983.

[9] K.E. Gregorich, et al., Actinide production in ^{136}Xe bombardments of ^{249}Cf, Phys. Rev. C 35 (1987) 2117–2124, https://doi.org/10.1103/PhysRevC.35.2117.

[10] K.J. Moody, et al., New nuclides: neptunium-243 and neptunium-244, Z. Phys. A 328 (1987) 417–422, https://doi.org/10.1007/BF01289627.

[11] R.M. Chasteler, et al., Excitation functions for production of heavy actinides from interactions of ^{16}O with ^{249}Cf, Phys. Rev. C 36 (1987) 1820–1825, https://doi.org/10.1103/PhysRevC.36.1820.

[12] K.J. Moody, et al., Actinide cross sections from the reaction of ^{13}C with ^{254}Es^{g}, Phys. Rev. C 41 (1990) 152–159, https://doi.org/10.1103/PhysRevC.41.152.

[13] A. Türler, et al., Actinide production from the interactions of ^{40}Ca and ^{44}Ca with ^{248}Cm and a comparison with the ^{48}Ca+^{248}Cm system, Phys. Rev. C 46 (1992) 1364–1382, https://doi.org/10.1103/PhysRevC.46.1364.

[14] V.F. Comas, et al., Study of multi-nucleon transfer reactions in ^{58,64}Ni+ ^{207}Pb collisions at the velocity filter SHIP, Eur. Phys. J. A 49 (2013) 1–17, https://doi.org/10.1140/epja/i2013-13112-x.

[15] O. Beliuskina, et al., On the synthesis of neutron-rich isotopes along the N = 126 shell in multinucleon transfer reactions, Eur. Phys. J. A 50 (2014) 161, https://doi.org/10.1140/epja/i2014-14161-3.

[16] H.M. Devaraja, et al., Observation of new neutron-deficient isotopes with Z≥92 in multinucleon transfer reactions, Phys. Lett. B 748 (2015) 199–203, https://doi.org/10.1016/j.physletb.2015.07.006.

[17] S. Heinz, et al., Synthesis of new transuranium isotopes in multinucleon transfer reactions using a velocity filter, Eur. Phys. J. A 52 (2016) 278, https://doi.org/10.1140/epja/i2016-16278-7.

[18] H.M. Devaraja, et al., Population of nuclides with Z≥98 in multi-nucleon transfer reactions of ^{48}Ca+ ^{248}Cm, Eur. Phys. J. A 55 (2019) 25, https://doi.org/10.1140/epja/i2019-12696-3.

[19] H.M. Devaraja, et al., New studies and a short review of heavy neutron-rich transfer products, Eur. Phys. J. A 56 (2020) 224, https://doi.org/10.1140/epja/s10050-020-00229-2.

[20] T. Niwase, et al., Discovery of new isotope ^{241}U and systematic high-precision atomic mass measurements of neutron-rich Pa-Pu nuclei produced via multinucleon transfer reactions, Phys. Rev. Lett. 130 (2023) 132502, https://doi.org/10.1103/PhysRevLett.130.132502.

[21] G.G. Adamian, et al., Production of unknown transactinides in asymmetry-exit-channel quasifission reactions, Phys. Rev. C 71 (2005) 034603, https://doi.org/10.1103/PhysRevC.71.034603.

[22] Zhao-Qing Feng, et al., Production of heavy isotopes in transfer reactions by collisions of ^{238}U+ ^{238}U, Phys. Rev. C 80 (2009) 067601, https://doi.org/10.1103/PhysRevC.80.067601.

[23] G.G. Adamian, et al., Predicted yields of new neutron-rich isotopes of nuclei with Z = 64–80 in the multinucleon transfer reaction ^{48}Ca+ ^{238}U, Phys. Rev. C 81 (2010) 057602, https://doi.org/10.1103/PhysRevC.81.057602.

[24] Zhao-Qing Feng, Production of neutron-rich isotopes around N = 126 in multinucleon transfer reactions, Phys. Rev. C 95 (2017) 024615, https://doi.org/10.1103/PhysRevC.95.024615.

[25] L. Zhu, Theoretical study on production cross sections of exotic actinide nuclei in multinucleon transfer reactions, Chin. Phys. C 41 (2017) 124102, https://doi.org/10.1088/1674-1137/41/12/124102.

[26] V. Zagrebaev, W. Greiner, Synthesis of superheavy nuclei: a search for new production reactions, Phys. Rev. C 78 (2008) 034610, https://doi.org/10.1103/PhysRevC.78.034610.

[27] V. Zagrebaev, W. Greiner, Production of new heavy isotopes in low-energy multinucleon transfer reactions, Phys. Rev. Lett. 101 (2008) 122701, https://doi.org/10.1103/PhysRevLett.101.122701.

[28] A.V. Karpov, V.V. Saiko, Modeling near-barrier collisions of heavy ions based on a Langevin-type approach, Phys. Rev. C 96 (2017) 024618, https://doi.org/10.1103/PhysRevC.96.024618.

[29] V.V. Saiko, A.V. Karpov, Analysis of multinucleon transfer reactions with spherical and statically deformed nuclei using a Langevin-type approach, Phys. Rev. C 99 (2019) 014613, https://doi.org/10.1103/PhysRevC.99.014613.

[30] A. Winther, Dissipation, polarization and fluctuation in grazing heavy-ion collisions and the boundary to the chaotic regime, Nucl. Phys. A 594 (1995) 203–245, https://doi.org/10.1016/0375-9474(95)00374-A.

[31] Ning Wang, et al., Improved quantum molecular dynamics model and its applications to fusion reaction near barrier, Phys. Rev. C 65 (2002) 064608, https://doi.org/10.1103/PhysRevC.65.064608.

[32] Cheng Li, et al., Multinucleon transfer in the ^{136}Xe +^{208} Pb reaction, Phys. Rev. C 93 (2016) 014618, https://doi.org/10.1103/PhysRevC.93.014618.

[33] Ning Wang, Lu Guo, New neutron-rich isotope production in ^{154}Sm+ ^{160}Gd, Phys. Lett. B 760 (2016) 236–241, https://doi.org/10.1016/j.physletb.2016.06.073.

[34] Cheng Li, et al., Production mechanism of new neutron-rich heavy nuclei in the ^{136}Xe+ ^{198}Pt reaction, Phys. Lett. B 776 (2018) 278–283, https://doi.org/10.1016/j.physletb.2017.11.060.

[35] K. Sekizawa, K. Yabana, Time-dependent Hartree-Fock calculations for multinucleon transfer processes in ^{40,48}Ca+ ^{124}Sn, ^{40}Ca+ ^{208}Pb, and ^{58}Ni+ ^{208}Pb reactions, Phys. Rev. C 88 (2013) 014614, https://doi.org/10.1103/PhysRevC.88.014614.

[36] K. Sekizawa, Microscopic description of production cross sections including deexcitation effects, Phys. Rev. C 96 (2017) 014615, https://doi.org/10.1103/PhysRevC.96.014615.

[37] M. Thoennessen, The Discovery of Isotopes, a Complete Compilation, Springer International Publishing, Cham, 2016.

[38] H. Jianjun, et al., Synthesis and identification of a new heavy neutron-rich isotope ^{238}Th, Phys. Rev. C 59 (1999) 520–521, https://doi.org/10.1103/PhysRevC.59.520.

[39] E.K. Hulet, et al., Spontaneous fission properties of ^{258}Fm, ^{259}Md, ^{260}Md, ^{258}No, and ^{260}104: bimodal fission, Phys. Rev. C 40 (1989) 770–784, https://doi.org/10.1103/PhysRevC.40.770.

[40] A.G. Popeko, et al., Separator for heavy ELement spectroscopy – velocity filter SHELS, Nucl. Instrum. Methods Phys. Res. B 376 (2016) 140–143, https://doi.org/10.1016/j.nimb.2016.03.045.

[41] R. Bass, Fusion of heavy nuclei in a classical model, Nucl. Phys. A 231 (1974) 45–63, https://doi.org/10.1016/0375-9474(74)90292-9.

[42] IAEA NDS interactive chart of nuclides, https://www-nds.iaea.org/relnsd/vcharthtml/VChartHTML.html. (Accessed 29 August 2024).

[43] V. Zagrebaev, et al., Potential energy of a heavy nuclear system in fusion-fission processes, Phys. Part. Nucl. 38 (2007) 469, https://doi.org/10.1134/S106377960704003X.

[44] A. Karpov, V. Saiko, Synthesis of transuranium nuclei in multinucleon transfer reactions at near-barrier energies, Phys. Part. Nucl. Lett. 16 (2019) 667–670, https://doi.org/10.1134/S1547477119060475.

[45] A. Yeremin, Prospects of investigation of multinucleon transfer reactions, in: Programme Advisory Committee for Nuclear Physics 51st Meeting, Dubna, Russia, 30–31 January 2020.

[46] M.I. Yavor, et al., Development of a mass spectrometer for high-precision mass measurements of superheavy elements at JINR, J. Instrum. 17 (2022) P11033, https://doi.org/10.1088/1748-0221/17/11/P11033.